HHS Public Access

Author manuscript

Leukemia. Author manuscript; available in PMC 2012 March 01.

Published in final edited form as:

Leukemia. 2011 September ; 25(9): 1484–1493. doi:10.1038/leu.2011.115.

The Immunoglobulin Heavy Chain Gene 3' Enhancers Induce *Bcl2* Deregulation and Lymphomagenesis in Murine B Cells

Hong Xiang, MD, PhD[1,2], **Emily J. Noonan, PhD**[1,2], **Jinghong Wang, PhD**[1,2], **Hong Duan, PhD**[1,2], **Lawrence Ma, BS**[1,2], **Sara Michie, MD**[3], and **Linda M. Boxer, MD, PhD**[1,2,*]

[1]Center for Molecular Biology in Medicine, Veterans Affairs Palo Alto Health Care System, Palo Alto, California 94304

[2]Department of Medicine, Stanford University School of Medicine, Stanford, California 94305

[3]Department of Pathology, Stanford University School of Medicine, Stanford, California 94305

Abstract

Human follicular B-cell lymphoma is associated with the t(14;18) chromosomal translocation that juxtaposes the *Bcl2* proto-oncogene with the immunoglobulin heavy chain (*Igh*) locus, resulting in the deregulated expression of *Bcl2*. Our previous studies have shown that the *Igh* 3' enhancers deregulate *Bcl2* expression *in vitro*. However, the effects of the *Igh* 3' enhancer elements on *Bcl2* expression *in vivo* are not known. To investigate the role of the *Igh* 3' enhancers in *Bcl2* deregulation, we used gene targeting to generate knock-in mice in which four DNase I hypersensitive regions from the murine *Igh* 3' region were integrated 3' of the *Bcl2* locus. Increased levels of *Bcl2* mRNA and protein were observed in the B cells of Igh-3'E-bcl2 mice. B cells from Igh-3'E-bcl2 mice demonstrated an extended survival *in vitro* compared with B cells from wild-type mice. The *Bcl2* promoter shift from P1 (the 5' promoter) to P2 (the 3' promoter) was observed in B cells from Igh-3'E-bcl2 mice, similar to human t(14;18) lymphomas. The IgH-3'E-bcl2 mice developed monoclonal B-cell follicular lymphomas, which were slowly progressive. These studies demonstrate that the *Igh* 3' enhancers play an important role in the deregulation of *Bcl2* and B-cell lymphomagenesis *in vivo*.

Keywords

lymphoma; Bcl2; t(14;18); *Igh* enhancer; mouse models

INTRODUCTION

Human follicular lymphoma is the most common low-grade non-Hodgkin's lymphoma (1), and most of these lymphomas are associated with the chromosomal translocation t(14;18).

*To whom correspondence should be addressed: Hematology, CCSR 1155, 269 Campus Drive, Stanford University School of Medicine, Stanford, CA 94305-5156, Tel.: 650-849-0551, Fax: 650-858-3982, lboxer@stanford.edu.

CONFLICT OF INTEREST

The authors declare no potential conflicts of interest with respect to the authorship and/or publication of this article.

One allele of the *Bcl2* gene on chromosome 18 is translocated to the immunoglobulin heavy chain (*Igh*) gene on chromosome 14. The translocation results in increased levels of BCL2 mRNA and protein (2–4), and the transcripts originate from the translocated allele, while the normal allele is silent (5). BCL2 plays an important role in the prevention of apoptosis, and the deregulated expression of *Bcl2* is required for the pathogenesis of follicular lymphoma.

Several transgenic mouse models expressing *Bcl2* under the control of an *Igh* intronic enhancer (Eμ) have been generated (6–8), and several of them develop B cell lymphomas, particularly in cooperation with *Myc* (9–11), although these are not models for low-grade human lymphoma. Another transgenic mouse model for exploring the tumorigenic potential of *Bcl2* has also been established with *Bcl2* expressed in all hematopoietic lineages (12–13). In addition, other mouse models of lymphoma using the *Igh* 3' enhancers or the *Igh* locus control region to drive expression of other oncogenes have been described, for example (14–15).

Two promoters mediate transcriptional control of the *Bcl2* gene. The 5' promoter (P1) is a major positive regulator in normal human B-cells, while the 3' promoter (P2) exhibits only low activity (5). Conversely in B lymphoma cells with the t(14;18) translocation, the P2 promoter is activated and becomes the major positive regulator (5, 16). The *Igh* 3' enhancers, which contain four B-cell specific DNase I-hypersensitive sites (HS1234), are located 16 kb 3' of the murine *Igh-C* α gene and 25 kb 3' of the human *IGHC* α gene (17–19). We have previously shown that the *Igh* 3' enhancers greatly increase human *Bcl2* P2 promoter activity and the shift from P1 to P2 promoter usage in an episomal construct, similar to the shift that is observed in t(14;18) lymphomas (20). Further, the addition of the *Igh* intronic switch enhancer with the IgH 3' enhancers *in vitro* did not result in any further deregulation of *Bcl2* expression. What is not known is whether the *Igh* 3' enhancers play an important role in the deregulation of *Bcl2 in vivo* or in the context of the native chromatin.

To study the mechanisms of *Bcl2* deregulation *in vivo*, we generated mice (IgH-3'E-bcl2) with the *Igh* 3' enhancers targeted 3' of the *Bcl2* gene and evaluated the expression of *Bcl2* and the effects on B cell development. Insertion of the *Igh* enhancers 3' of the *Bcl2* gene preserved the great distance between the *Igh* enhancer and the *Bcl2* promoter which resulted in increased levels of BCL2, prolonged the survival of B cells, and promoted tumorigenesis. The IgH-3'E-bcl2 mice developed B-lymphoid malignancies with similarities to human low-grade lymphoma.

MATERIALS AND METHODS

Construction of the targeting vector

A mouse genomic *Bcl2* BAC clone from a 129/J library (Incyte Genomics, Wilmington, DE) was utilized for construction of the targeting vector. A 2.5 kb EcoRI fragment 3' of the *bcl*-2 3' UTR was isolated from the *Bcl2* BAC clone as the short arm of the vector. A 1.7 kb AseI-AflII fragment including the *Bcl2* coding region, a 3.14 kb AflII-EcoRI fragment, and a 1.3 kb EcoRI fragment were isolated from the *Bcl2* BAC clone, subcloned, and ligated to form a 6.1kb fragment as the long arm. To generate the targeting vector, the 2.5-kb EcoRI fragment was blunt-ended and inserted into the pPNT-loxP vector 3' of the neomycin cassette. The

6.1-kb fragment was inserted 5’ of the neomycin cassette. Finally, a 4.2-kb fragment containing the four DNase I hypersensitive sites of the murine *Igh* 3' enhancers (IgH-3'E) was inserted between the 6.1-kb long arm and the neomycin cassette.

Generation of IgH-3'E-bcl2 knock-in mice

R1 ES (129/J) cells were electroporated with the linearized targeting vector, selected with G418 and ganciclovir, and screened by PCR using a neomycin primer and a primer 5' to the construct arm. Recombinant ES clones were confirmed by Southern blot analysis with a probe containing genomic sequences 5' to the long construct arm. Two targeted clones were injected into C57BL/6 blastocysts. Germ line transmission was confirmed by long-distance PCR on mouse tail DNA with a primer, LD-B, from the *Bcl2* region and another primer, LD-N, from the neomycin cassette to amplify a 3.0-kb fragment (see Supplementary Table 1 for primer sequences). Two different mouse lines were characterized, and no differences were observed between them. It is important to note that there is a large intron present in the mouse Bcl2 gene, and therefore the *Igh* enhancers will be located approximately 170 kb 3’ of the *Bcl2* promoter in the targeted allele. The neomycin-IgH-3'E-bcl2 mice were bred with mice carrying a transgene expressing the Cre recombinase under the control of the β-actin promoter (21) to remove the neomycin cassette and generate IgH-3'E-bcl2 knock-in mice.

Genotyping was performed using two sets of primers. PCR with primer A (GEN-A) from the *Bcl2* gene and primer B (GEN-B) from the *Igh* 3’ enhancer region amplified a 480-bp fragment from the IgH-3’E-bcl2 mice. PCR was performed with primer A and primer C (GEN-C) from the sequence of the *Bcl2* gene to amplify a 620-bp fragment from wild-type mice (see Supplementary Table 1 for primer sequences).

Immunofluorescence staining and flow cytometric analysis

Cells from spleen and bone marrow were depleted of erythrocytes with RBC lysis buffer (eBioscience, San Diego CA), and then washed with cold phosphate-buffered saline (PBS) containing 5% bovine serum albumin and 0.1% sodium azide. Approximately 1×10^6 cells were stained with different fluorescein isothiocyanate (FITC)-, phycoerythrin (PE)-, and allophycocyanin (APC)-conjugated antibodies to cell surface markers (BD Pharmingen, San Diego CA). The following anti-mouse mAbs were used: PE-conjugated anti-CD19, FITC-conjugated anti-CD3, PE-conjugated anti-B220, APC-conjugated anti-IgM, FITC-conjugated anti-IgD, FITC-conjugated anti-B220, PE-conjugated anti-CD43. Cell viability was determined using 7-amino-actinomycin (7-AAD, eBioscience). Cells were analyzed in a FACSCalibur flow cytometer with Cell Quest software (BD Biosciences, Franklin Lakes, NJ). Pro-B ($B220^+IgM^-CD43^+$), pre-B ($B220^+IgM^-CD43^-$), immature B cells ($B220^+IgM^+IgD^-$) and mature B cells ($B220^+IgM^+IgD^+$) were identified.

PCR assay for clonality

Genomic DNA was isolated from B cells of spleens and enlarged lymph nodes of IgH-3’E-bcl2 mice. PCR was performed using primers that detect rearrangements of diversity and joining (D-J) regions from *Igh* genes (22–24). The DSF primer anneals to a region 5’ to most murine DH genes and the JH4 primer anneals to an intronic region 3’ of the JH4 gene. Clonal Ig rearrangements were identified by the intensity and presence of different

molecular weight bands compared to a splenic polyclonal control. *Igh* Variable and D-J (V-D-J) sequences from selected monoclonal or oligoclonal lymphoma samples were then amplified by high fidelity PCR using Pfx polymerase (Invitrogen, Carlsbad CA), a set of degenerate primers specific to the FR1 region of V genes (MH1-7) and a nested primer 3' to JH4 (JHR) (12, 25). PCR was performed in two rounds using an annealing temperature of 63°C for 30 cycles with equimolar concentration of all MH1-7 primers with JHR in the first round and individual MH primers with JHR in the second round (see Supplementary Table 1 for primer sequences). Fragments were gel purified and cloned into a pGEM-Teasy vector (Promega, Madison, WI). VDJ gene usage was determined by Ig BLAST database (www.ncbi.nlm.nih.gov/igblast) using the lowest penalty to match longer stretches of sequence. *Igh* gene sequence was compared to germline DNA sequences using the IMGT database to determine percent somatic hypermutation (26).

Primer extension

The location of the transcription initiation sites of the mouse *Bcl2* gene were determined by primer extension analysis with Primer Extension System (Promega) following the manufacturer's instructions. Two oligonucleotide antisense primers were used in the extension reaction. Primer E3 (Oligo A) was used to map upstream start sites, and primer E2 (Oligo B) was used to map the downstream start sites. ^{32}P-end-labeled primer was annealed to 0.5 μg poly(A)+ RNA extracted from B cells using the Micro-Fast Track mRNA isolation kit (Invitrogen). Yeast transfer RNA (Ambion, Foster City, CA) served as a negative control. The extension products and a sequencing ladder generated with the same primers were analyzed by electrophoresis on an 8% polyacrylamide, 7M urea gel. The putative sites of transcription initiation were determined by comparison with Φχ174 DNA/Hinf I dephosphorylated marker (see Supplementary Table 1 for primer sequences).

Histology and Immunohistology

Lymph nodes and spleens from IgH-3'E-bcl2 and wild type (Wt) mice were fixed in formalin for histologic evaluation or frozen in OCT compound for immunoperoxidase/DAB staining. Methods, reagents, interpretation and photomicroscopy are described in the Supplementary Information.

Promoter usage analysis

Transcripts from the mouse *Bcl2* P1 promoter and total transcripts (from both P1 and P2 promoters) were determined by real-time PCR. Total RNA was isolated from purified B cells with the RNeasy mini kit (QIAGEN, Valencia, CA) with additional DNAse digestion, precipitated in 2.5M LiCl, and reverse-transcribed to cDNA with a RETROscript kit (Ambion). Real-time PCR was performed using the 7900HT Real-Time System (Applied Biosystems, Foster City, CA) in conjunction with specific primer/probe sets for the detection of transcripts originating from the P1 promoter and total *Bcl2* transcripts (P total), which detects transcripts from both promoters. Absolute quantification of transcripts originating from the P2 promoter was estimated using digital PCR to determine the mRNA copy number of both P1 and P total transcripts.

Chromosome conformation capture (3C) assay

The 3C assay was carried out as previously described with a few modifications to examine the association of the *Igh* 3' enhancer region with the *Bcl2* locus (27–28). Briefly, lymphoma cells were purified using the B cell isolation kit from Miltenyi. Purified cells were fixed with 1% formaldehyde and quenched by addition of 0.125 M glycine. Nuclei were isolated and digested with BamHI overnight (>80% digestion), followed by ligation for 5 hours using T4 DNA ligase (New England Biolabs, Ipswich, MA). The ligation product was further treated with proteinase K and purified by phenol/chloroform extraction. The purified 3C DNA was quantified by TaqMan primer/probe based real-time PCR. Real-time PCR was performed on the ABI Prism 7900-HT Sequence Detection System using the Universal PCR Master Mix (Applied Biosystems). The absolute PCR signal was further normalized to primer/probe efficiency using control 3C template generated from equal molar PCR fragments using homologous PCR primers. The relative association was represented as the average and standard deviation from three independent 3C analyses. For the design of PCR primer/probe, the anchor primer (Anch-IgH) and probe (Anch-IgH-probe) were chosen from the *Igh* locus and the other primers were chosen from the *Bcl2* locus, 5' and 3' of the *Bcl2* translation start site. All the primers and the probe were chosen from the sequences 5' of BamHI site. The Ercc3 locus was utilized for normalization of the 3C associations because it has been shown to adopt similar chromosome conformations in different mouse tissues by 3C analysis (29). The location of the *Bcl2* primers relative to the *Bcl2* translation start site (which is defined as 0) is shown in parentheses (see Supplementary Table 1 for primer sequences).

For methods not included within the manuscript, see supplementary information.

RESULTS

Generation of IgH-3'E-bcl2 knock-in mice

IgH-3'E-bcl2 knock-in mice were generated by insertion of the four DNase I hypersensitive sites of the murine *Igh* 3' enhancers (HS1234) into the *Bcl2* locus in murine embryonic stem (ES) cells by homologous recombination (Figure 1A). Targeted ES cells were identified by PCR and Southern blot analysis using a probe from outside of the region of homology (Figure 1B). Germ line transmission was confirmed by long-distance PCR of mouse tail DNA (Figure 1C). The neomycin cassette flanked by loxP sites in the neomycin-IgH-3'E-bcl2 mice was removed by breeding with transgenic mice expressing the Cre recombinase under the control of the β-actin promoter, and the mice were genotyped by PCR. The mice with neomycin deleted are designated as IgH-3'E-bcl2 mice.

Expression of *Bcl2* in IgH-3'E-bcl2 mice

The levels of *Bcl2* mRNA and protein were examined in different tissues of the IgH-3'E-bcl2 mice. As shown in Figure 2A, *Bcl2* mRNA levels were increased in the spleens of IgH-3'E-bcl2 mice as compared with wild-type mice. Expression of *Bcl2* in spleens from homozygous IgH-3'E-bcl2 mice was greater than that of heterozygous mice. The level of expression of *Bcl2* in thymus, lung, kidney, and liver from IgH-3'E-bcl2 mice was not different from that of wild-type mice (Figure 2A). In order to determine if the origin of

elevated *Bcl2* expression in the spleen was B-cell specific, B lymphocytes and non-B-cell populations isolated from spleens of IgH-3'E-bcl2 and wild-type mice were compared. Relative to wild type mice, *Bcl2* transcripts isolated from IgH-3'E-bcl2 mice were increased in B cells (Figure 2B) but not in non-B cells (data not shown). BCL2 protein levels in purified splenic B cells from IgH-3'E-bcl2 mice were 3.5- to 5.5-fold higher compared to B cells from wild-type mice (Figure 2C). These results demonstrate that increased expression of *Bcl2* is restricted to B lymphocytes in IgH-3'E-bcl2 mice.

Altered B cell differentiation in IgH-3'E-bcl2 mice

To determine whether there were changes in the B-cell populations of IgH-3'E-bcl2 mice, freshly purified lymphocytes from bone marrows and spleens were stained with different combinations of antibodies to cell surface markers including CD19, CD3, B220, CD43, IgM, and IgD, and analyzed by flow cytometry. Increased numbers of B cells ($CD19^+$) were observed in both bone marrow and spleen compared to those of wild-type mice (Figure 3A). The $B220^+IgM^+IgD^-$ and $B220^+IgM^+IgD^+$ immature and mature B cells were increased in both bone marrow and spleens of IgH-3'E-bcl2 mice (Figure 3B and C). In the bone marrow, an increase in the percentage of $B220^+CD43^-IgM^-$ (pre-B) cells was observed, while there was no change in the percentage of $B220^+CD43^+IgM^-$ (pro-B) cells (Figure 3D). T-cell populations in the peripheral blood of IgH-3' Bcl2 were quantified and showed no change in absolute number or in the ratio of $CD4^+$ to $CD8^+$ T cells compared to wild type mice (data not shown). These data indicate that B lymphoid homeostasis was perturbed in IgH-3'E-bcl2 mice resulting in an expansion of pre-B, immature, and mature B cells due to overexpressed BCL2.

Progression through the cell cycle is delayed in B cells from IgH-3'E-bcl2 mice

To investigate the effect of overexpressed BCL2 on the cell cycle, we purified B lymphocytes from spleens of IgH-3'E-bcl2 mice and control littermates, and cultured the B cells with 5 μg/ml of anti-CD40. Cells were collected at 12, 24, and 48 h, stained with propidium iodide-RNase A solution, and analyzed by flow cytometry for relative DNA content. Results were collected in triplicate and representative plots are shown. At the 0 h time point, the majority (approximately 97%) of control and IgH-3'E-bcl2 B cells were in the G0/G1 phase (Figure 4). Following treatment with anti-CD40 for 12 h, control B cells from wild-type mice showed a significant increase in the percentage of cells in the S-G2/M phases, while the B cells from IgH-3'E-bcl2 mice remained in the G0/G1 phase (Figure 4). After 24 and 48 h of stimulation, B cells from IgH-3'E-bcl2 mice displayed 2.5- to 3.5-fold fewer cells in the S-G2/M phases of the cell cycle as compared with B cells from control mice (Figure 4). These results demonstrate that over-expressed BCL2 delayed the transition from G0/G1 to S-G2/M in B cells.

B cells from IgH-3'E-bcl2 mice show increased viability

To examine the effect of increased BCL2 expression on the survival of B cells from IgH-3'E-bcl2 mice, cell viability in culture was measured every 24 hours up to 3 days. As shown in Figure 5A, the B cells from IgH-3'E-bcl2 mice remained viable for longer periods of time compared to B cells from wild-type mice. The B cells from homozygous IgH-3'E-

bcl2 mice survived longer than those from heterozygous mice. Additionally, specific B-cell populations isolated from both the bone marrow and the spleen including $B220^{+}CD43^{-}IgM^{-}$ (pre-B) cells, $B220^{+}IgM^{+}IgD^{-}$ (immature), and $B220^{+}IgM^{+}IgD^{+}$ (mature) B-cells from IgH-3'E-bcl2 mice all exhibited increased viability at 24 hours compared to wild type (Figure 5B). The viability of $B220^{+}CD43^{+}IgM^{-}$ (pro-B) cells from IgH-3'E-bcl2 mice was similar to that from wild type mice (Figure 5B).

Development of B cell lymphomas in IgH-3'E-bcl2 mice

Splenomegaly was observed in the IgH-3'E-bcl2 mice at approximately 4 months of age, and it was more pronounced in homozygous compared to heterozygous mice. At 10 to 12 months of age, heterozygous IgH-3'E-bcl2 mice had spleens 6 to 10 times the weight of wild-type littermates and lymph nodes 5 to 10 times larger than those of wild-type mice. Histologic sections of large lymph nodes from 7 to 14 month old IgH-3'E-bcl2 mice (n=20) revealed follicular lymphoma (Figure 6A). In 18 of 20 mice, >90% of the lymphoma area had a follicular pattern (Figure 6A). Frozen section immunohistology stains for B cell antigens (Figures 6B and 6C) and germinal center markers (Figures 6D and 6E) highlighted the lymphoma follicles. Most of the lymphoma cells were small, with irregular nuclear outlines, hyperchromatic chromatin and occasional small nucleoli (Figure 6A inset). There were scattered large cells with open chromatin and prominent nuclei (Figure 6A inset). As in human follicular lymphoma, there were T cells between and within the follicles (Figure 6F and 6G) and follicular dendritic cells in most follicles (not shown). Supplementary Figure 1 shows a normal lymph node from a wild type mouse for comparison. Histology (n=20) and immunohistology (n=6) stains of IgH-3'E-bcl2 spleens revealed extensive involvement of white pulp by B cell lymphoma (not shown). There was also an increase in the number of plasma cells in the large lymph nodes and spleens. Clonality studies revealed that the plasma cells were polyclonal (data not shown).

PCR analysis was performed to assess clonality in B cell populations isolated from enlarged lymph nodes of IgH-3'E-bcl2 mice. Genomic DNA was extracted and amplified using primers that detect rearrangements of diversity and joining (D-J) regions from *Igh* genes. Monoclonal populations were identified by the presence of a single band compared to a splenic polyclonal control. VDJ sequences from genomic DNA of selected monoclonal or oligoclonal lymphoma samples were then PCR amplified using a set of degenerate primers and sequenced. PCR analysis of the *Igh* rearrangements from lymphomas of heterozygous IgH-3'E-bcl2 mice revealed that they were monoclonal. Clonality results of two different lymphomas are shown in Figure 7. Compared to multiple rearranged bands in a polyclonal splenic control (Figure 7A lanes 1–7), only one rearranged band was observed with the DNA from lymphomas (Figure 7B lane 6, Figure 7C lane 5). Sequencing results showed that a number of different *Igh* genes were utilized, and the *Igh* genes from lymphoma samples had undergone somatic hypermutation with a deviation for samples >2% compared to germline (30–31). Preliminary results revealed evidence for intraclonal *Ighv* gene diversification in several lymphoma samples that were analyzed (data not shown).

Forty-seven heterozygous IgH-3'E-bcl2, and thirty-five wild-type littermates were observed to record their lifespan. The IgH-3'E-bcl2 mice have significantly decreased survival when

compared with wild-type littermates (Figure 7D). The average age of death is approximately 55 weeks (~1 year) for the heterozygous IgH-3'E-bcl2 mice. Homozygous IgH-3'E-bcl2 mice also developed lymphomas similar to the ones observed in heterozygous mice with hastened onset of disease (several weeks). Although these were not extensively characterized because the heterozygous IgH-3'E-bcl2 mice represent a more accurate molecular model for t(14;18) lymphomas.

The *Bcl2* promoter shift from P1 to P2 is observed in lymphoma cells from IgH-3'E-bcl2 mice

The transcription initiation sites for *Bcl2* were mapped in B cells from IgH-3'E-bcl2 mice to determine whether the P2 promoter was activated by the *Igh* enhancers. Primer extension revealed that both the P1 and P2 promoters were active in lymphoma cells from homozygous IgH-3'E-bcl2 mice (Figure 8A and B). Real-time PCR was performed with wild-type B cells and B cells from homozygous IgH3'E-bcl2 mice at a range of 1–12 months of age. (Homozygous mice were used to assess promoter usage to eliminate background from the untargeted *Bcl2* allele.) As expected, transcripts initiated predominantly at the P1 promoter in wild-type B cells (P2 to P1 ratio of approximately 0.1 to 0.25, Figure 8C). Interestingly, there was essentially no change in promoter usage in B cells from young (<1 month of age) IgH-3'E-bcl2 mice. However, the P2 promoter was activated in B cells from older IgH-3'E-bcl2 mice, and the P2 to P1 ratio increased to 1.6 to 2.4 (Figure 8C). These results are similar to the promoter shift that is observed in human follicular lymphoma cells (20).

The IgH enhancers interact with the *Bcl2* promoter

It is likely that the *Igh* enhancers are responsible for the increased transcription of B*cl*2 and for the promoter shift in lymphoma cells from homozygous IgH-3'E-bcl2 mice. The *Igh* enhancers are located over 170 kb 3' of the *Bcl2* promoter in the IgH-3'bcl2 mice so we wished to determine whether the targeted *Igh* enhancers interact with the *Bcl2* promoter. Chromosome conformation capture analysis was performed with B cells from wild-type mice and with lymphoma cells from the IgH-3'E-bcl2 mice. We did not observe any association of the *Igh* enhancer with the *Bcl2* locus in B cells from the wild-type mice (data not shown). Interactions of the *Igh* 3' enhancer sequence with the *Bcl2* locus were detected in lymphoma cells (Figure 9). The interaction signals decrease with the increasing distance from the *Bcl2* promoter regions (the region near 0 on the x axis in Figure 9), suggesting that the interactions are functionally related.

DISCUSSION

The t(14;18) translocation results in inappropriately elevated levels of *Bcl2* in human follicular lymphoma. The *Igh* 3' enhancers are believed to play a role in the increased expression of *Bcl2* in t(14;18) lymphoma cells. Our previous *in vitro* studies showed that the four DNase I-hypersensitive regions (HS1234) of the *Igh* 3' enhancers up-regulated *Bcl2* expression (20, 32). We have now established a mouse model of the t(14;18) by targeting the *Igh* 3' enhancers to the *Bcl2* gene in murine ES cells. This approach avoids positional

and copy number effects and reproduces the great linear distance between the *Igh* enhancers and the *Bcl2* promoter.

The IgH-3'E-bcl2 mice exhibited significantly increased expression levels of *Bcl2* mRNA and protein in B cells but not in other cells, including T cells. Increased numbers of pre-B, immature, and mature B cells are observed in the mice, and the B cells are polyclonal. This is similar to observations in transgenic models of over-expressed *Bcl2*. As has been described by others in different model systems, increased levels of BCL2 delayed entry and progression through the cell cycle in B cells from Igh-3'E-bcl2 mice (33–35). The B cells from IgH-3'E-bcl2 also survived for longer periods in culture compared to wild-type B cells.

Monoclonal B cell lymphomas developed as the IgH-3'E-bcl2 mice aged. Histologic analysis of the enlarged lymph nodes and spleens revealed extensive infiltrates of small lymphocytes with irregular nuclear outlines and hyperchromatic chromatin. The vast majority of the lymph nodes showed a follicular pattern. Many studies indicate that non-neoplastic cells in the tumor microenvironment are important in development, proliferation, and response to therapy of human follicular lymphomas (36–39). The follicular lymphomas in the IgH-3'E-bcl2 mice contain T cells (CD4+>CD8+) and follicular dendritic cells, as do human follicular lymphomas. The lymphoma cells in the IgH-3'E-bcl2 mice express B cell antigens and germinal center markers as do the cells in human follicular lymphomas.

To determine whether the targeted *Igh* enhancers reproduced the molecular features of *Bcl2* deregulation observed in t(14;18) lymphomas, we examined *Bcl2* promoter usage in the lymphoma cells from IgH-3'E-bcl2 mice. We found that both *Bcl2* promoters were activated, but the activity of the P2 promoter increased significantly more than the activity of the P1 promoter did. This result is similar to our observations of increased P2 promoter activity from the translocated *Bcl2* allele in human t(14;18) lymphoma cells (20). The mechanisms of the induction of the *Bcl2* promoter shift are not entirely clear. Our previous studies have shown that NF-κB and Cdx sites in the *Igh* enhancers are involved in the activation of the P2 promoter (20). We have recently shown that the *Igh* 3' enhancers interact with the *Bcl2* promoter region in human t(14;18) lymphoma cells (40). We utilized chromosome conformation capture to determine whether the targeted *Igh* enhancers interact with the *Bcl2* promoter in lymphoma cells from IgH-3'E-bcl2 mice as this interaction is an important component of the transcriptional regulation of *Bcl2* in human follicular lymphoma cells. Using a primer from the *Igh* enhancer region, we observed increased interactions of this region with the *Bcl2* promoter. This interaction was not observed in B cells from wild-type mice. These results suggest that the targeted *Igh* enhancers interact and influence transcription from the *Bcl2* promoter in a manner similar to that observed in t(14;18) lymphoma cells.

The IgH-3'E-bcl2 mice differ from other mouse models of *Bcl2* over-expression in several important ways. *Bcl2* up-regulation is restricted to B cells in the IgH-3'E-bcl2 mice while this is not the case for many of the other models where BCL2 is often expressed in T cells as well as B cells. In fact, the T cells that over-express BCL2 were required for the development of lymphoma in the vav-bcl-2 mice (12). Most of the transgenic *Bcl2* mice show expansions of polyclonal B cells, and the mice develop aggressive lymphomas. One

possible explanation for the difference between these mice and the IgH-3'E-bcl2 mice is the fact that very high expression of BCL2 is induced in the transgenic mice (often 10- to 30-fold above normal), while the level of expression of BCL2 is 3- to 4-fold above that of wild type in the heterozygous IgH-3'E-bcl2 mice and approximately 5- to 6-fold higher in homozygous IgH-3'bcl2 mice. BCL2 interacts with other BH3 proteins, and its level of expression is clearly important in determining whether cells undergo apoptosis. It is possible that the lower level of BCL2 allows cells with major genetic changes to undergo apoptosis and slows the outgrowth of aggressive lymphomas. Strain differences may also be important. BCL2 expression is increased at the pre-B cell stage in IgH-3'E-bcl2 mice, and pre-B and more mature B cells show prolonged survival compared to B cells from wild type mice. It is not clear why malignancies of only mature B cells are observed, but this may reflect the requirement for cooperating mutations that are unique to the mature B cell stage of development.

In summary, we have demonstrated that the *Igh* 3' enhancers deregulate *Bcl2* expression and induce lymphomagenesis in murine B cells. There are many features of the lymphomas in the IgH-3'E-bcl2 mice that are similar to human low-grade lymphoma. The IgH-3'E-bcl2 mice provide a model to elaborate the mechanisms of *Bcl2* deregulation by the *Igh* enhancers and to study the development of lymphoma. A model that recapitulates the mechanisms involved in the tumorigenesis of low grade lymphoma will allow for testing of better chemotherapeutic treatment regimens.

Supplementary Material

Refer to Web version on PubMed Central for supplementary material.

ACKNOWLEDGEMENTS

We would like to thank Evelyn Resurreccion from Stanford University for her help and expertise with sectioning and immunohistochemical staining. This work was supported by National Institutes of Health Grant CA56764.

REFERENCES

1. Yunis JJ, Oken MM, Kaplan ME, Ensrud KM, Howe RR, Theologides A. Distinctive chromosomal abnormalities in histologic subtypes of non-Hodgkin's lymphomas. N Engl J Med. 1982; 307:1231. [PubMed: 7133054]
2. Cleary ML, Smith SD, Sklar J. Cloning and structural analysis of cDNAs for bcl-2 and a hybrid bcl-2/Immunoglobulin transcript resulting from the t(14;18) translocation. Cell. 1986; 47:19–28. [PubMed: 2875799]
3. Graninger WB, Seto M, Boutain B, Goldman P, Korsmeyer SJ. Expression of bcl-2 and bcl-2-Ig fusion transcripts in normal and neoplastic cells. J Clin Invest. 1987; 80:1512–1515. [PubMed: 3500184]
4. Tsujimoto Y, Croce C. Analysis of the structure, transcripts, and protein products of bcl-2, the gene involved in human follicular lymphoma. Proc Natl Acad Sci. 1986; 83:5214–5218. [PubMed: 3523487]
5. Seto M, Jaeger U, Hockett RD, Graninger W, Bennett S, Goldman P, et al. Alternative promoters and exons, somatic mutation and deregulation of the Bcl-2-Ig fusion gene in lymphoma. EMBO J. 1988; 7:123–131. [PubMed: 2834197]

6. Katsumata M, Siegel RM, Louie DC, Miyashita T, Tsujimoto Y, Nowell PC, et al. Differential effects of Bcl-2 on T and B cells in transgenic mice. Proc Natl Acad Sci USA. 1992; 89:11376–11380. [PubMed: 1454823]
7. McDonnell TJ, Deane N, Platt FM, Nunez G, Jaeger U, McKearn JP, et al. Bcl-2-immunoglobulin transgenic mice demonstrate extended B cell survival and follicular lymphoproliferation. Cell. 1989; 57:79–88. [PubMed: 2649247]
8. Strasser A, Whittingham S, Vaux DL, Bath ML, Adams JM, Cory S, et al. Enforced bcl-2 expression in B-lymphoid cells prolongs antibody responses and elicits autoimmune disease. Proc Natl Acad Sci USA. 1991; 88:8661–8665. [PubMed: 1924327]
9. McDonnell TJ, Korsmeyer SJ. Progression from lymphoid hyperplasia to high-grade malignant lymphoma in mice transgenic for the t(14;18). Nature. 1991; 349:254–256. [PubMed: 1987477]
10. Strasser A, Harris AW, Bath ML, Cory S. Novel primitive lymphoid tumours induced in transgenic mice by cooperation between myc and bcl-2. Nature. 1990; 348:331–333. [PubMed: 2250704]
11. Strasser A, Harris AW, Cory S. Em-bcl-2 transgene facilitates spontaneous transformation of early pre-B and immunoglobulin-secreting cells but not T cells. Oncogene. 1993; 8:1–9. [PubMed: 8423986]
12. Egle A, Harris AW, Bath ML, O'Reilly L, Cory S. VavP-Bcl2 transgenic mice develop follicular lymphoma preceded by germinal center hyperplasia. Blood. 2004; 103(6):2276–2283. [PubMed: 14630790]
13. Ogilvy S, Metcalf D, Print CG, Bath ML, Harris AW, Adams JM. Constitutive Bcl-2 expression throughout the hematopoietic compartment affects multiple lineages and enhances progenitor cell survival. Proc Natl Acad Sci USA. 1999; 96(26):14943–14948. [PubMed: 10611317]
14. Fiancette R, Amin R, Truffinet V, Vincent-Fabert C, Cogne N, Cogne M, et al. A myeloma translocation-like model associating CCND1 with the immunoglobulin heavy-chain locus 3' enhancers does not promote by itself B-cell malignancies. Leuk Res. 2010 Aug; 34(8):1043–1051. [PubMed: 20018375]
15. Truffinet V, Pinaud E, Cogne N, Petit B, Guglielmi L, Cogne M, et al. The 3' IgH locus control region is sufficient to deregulate a c-myc transgene and promote mature B cell malignancies with a predominant Burkitt-like phenotype. J Immunol. 2007 Nov 1; 179(9):6033–6042. [PubMed: 17947677]
16. Wu Y, Mehew JW, Heckman CA, Arcinas M, Boxer LM. Negative regulation of bcl-2 expression by p53 in hematopoietic cells. Oncogene. 2001; 20:240–251. [PubMed: 11313951]
17. Dariavach F, Williams GT, Campbell K, Pettersson S, Neuberger MS. The mouse IgH 3' enhancer. Eur J Immunol. 1991; 21:1499–1504. [PubMed: 1904361]
18. Madisen L, Groudine M. Identification of a locus control region in the immunoglobulin heavy-chain locus that deregulates c-myc expression in plasmacytoma and Burkitt's lymphoma cells. Gene & Devel. 1994; 8:2212–2226.
19. Pettersson S, Cook GP, Bruggemann M, Williams GT, Neuberger MS. A second B cell-specific enhancer 3' of the immunoglobulin heavy chain locus. Nature. 1990; 344:165–168. [PubMed: 2106628]
20. Duan H, Heckman CA, Boxer LM. The immunoglobulin heavy-chain gene 3' enhancers deregulate *bcl*-2 promoter usage in t(14;18) lymphoma cells. Oncogene. 2007; 26:2635–2641. [PubMed: 17043638]
21. Lewandoski M, Meyers EN, Martin GR. Analysis of Fgf8 gene function in vertebrate development. Cold Spring Harbor Symp Quant Biol. 1997; 62:159–168. [PubMed: 9598348]
22. Hoyer KK, French SW, Turner DE, Nguyen MT, Renard M, Malone CS, et al. Dysregulated TCL1 promotes multiple classes of mature B cell lymphoma. Proc Natl Acad Sci U S A. 2002 Oct 29; 99(22):14392–14397. [PubMed: 12381789]
23. Kawamoto H, Ikawa T, Ohmura K, Fujimoto S, Katsura Y. T cell progenitors emerge earlier than B cell progenitors in the murine fetal liver. Immunity. 2000 Apr; 12(4):441–450. [PubMed: 10795742]
24. Chang Y, Paige CJ, Wu GE. Enumeration and characterization of DJH structures in mouse fetal liver. EMBO J. 1992 May; 11(5):1891–1899. [PubMed: 1582417]

25. Wang Z, Raifu M, Howard M, Smith L, Hansen D, Goldsby R, et al. Universal PCR amplification of mouse immunoglobulin gene variable regions: the design of degenerate primers and an assessment of the effect of DNA polymerase 3' to 5' exonuclease activity. J Immunol Methods. 2000; 233:167–177. [PubMed: 10648866]
26. Lefranc MP, Giudicelli V, Kaas Q, Duprat E, Jabado-Michaloud J, Scaviner D, et al. IMGT, the international ImMunoGeneTics information system. Nucleic Acids Res. 2005 Jan 1; 33(Database issue):D593–D597. [PubMed: 15608269]
27. Dekker J, Rippe K, Dekker M, Kleckner N. Capturing chromosome conformation. Science. 2002; 295:1306–1311. [PubMed: 11847345]
28. Hagege H, Klous P, Braem C, Splinter E, Dekker J, Cathala G, et al. Quantitative analysis of chromosome conformation capture assays (3C-qPCR). Nature Protocols. 2007; 2(7):1722–1733. [PubMed: 17641637]
29. Zhou G-L, Xin L, Song W, Di L-J, Liu G, Wu X-S, et al. Active chromatin hub of the mouse a-globin locus forms in a transcription factory of clustered housekeeping genes. Mol Cell Biol. 2006; 26(13):5096–5105. [PubMed: 16782894]
30. Kienle D, Krober A, Katzenberger T, Ott G, Leupolt E, Barth TF, et al. VH mutation status and VDJ rearrangement structure in mantle cell lymphoma: correlation with genomic aberrations, clinical characteristics, and outcome. Blood. 2003 Oct 15; 102(8):3003–3009. [PubMed: 12842981]
31. Tracey L, Aggarwal M, Garcia-Cosio M, Villuendas R, Algara P, Sanchez-Beato M, et al. Somatic hypermutation signature in B-cell low-grade lymphomas. Haematologica. 2008 Aug; 93(8):1186–1194. [PubMed: 18556400]
32. Heckman CA, Cao T, Somsouk L, Duan H, Mehew JW, Zhang C, et al. Critical elements of the immunoglobulin heavy chain gene enhancers for deregulated expression of *bcl*-2. Cancer Res. 2003; 63:6666–6673. [PubMed: 14583460]
33. Greider C, Chattopadhyay A, Parkhurst C, Yang E. BCL-xL and BCL2 delay Myc-induced cell cycle entry through elevation of p27 and inhibition of G1 cyclin-dependent kinases. Oncogene. 2002; 21:7765–7775. [PubMed: 12420213]
34. Janumyan YM, Sansam CG, Chattopadhyay A, Cheng N, Soucie EL, Penn LZ, et al. Bcl-xL/ Bcl-2 coordinately regulates apoptosis, cell cycle arrest and cell cycle entry. EMBO J. 2003; 22(20): 5459–5470. [PubMed: 14532118]
35. O'Reilly LA, Huang DCS, Strasser A. The cell death inhibitor Bcl-2 and its homologues influence control of cell cycle entry. EMBO J. 1996; 15(24):6979–6990. [PubMed: 9003774]
36. Dave SS, Wright G, Tan B, Rosenwald A, Gascoyne RD, Chan WC, et al. Prediction of survival in follicular lymphoma based on molecular features of tumor-infiltrating immune cells. NEJM. 2004; 351(21):2159–2169. [PubMed: 15548776]
37. de Jong D, Koster A, Hagenbeek A, Raemaekers J, Veldhuizen D, Heisterkamp S, et al. Impact of the tumor microenvironment on prognosis in follicular lymphoma is dependent on specific treatment protocols. Haematologica. 2009 Jan; 94(1):70–77. [PubMed: 19059937]
38. Petrasch S, Kosco M, Perez-Alvarez C, Schmitz J, Brittinger G. Proliferation of non-Hodgkin-lymphoma lymphocytes in vitro is dependent upon follicular dendritic cell interactions. Br J Haematol. 1992 Jan; 80(1):21–26. [PubMed: 1536807]
39. Wahlin BE, Sander B, Christensson B, Kimby E. CD8+ T-cell content in diagnostic lymph nodes measured by flow cytometry is a predictor of survival in follicular lymphoma. Clin Cancer Res. 2007 Jan 15; 13(2 Pt 1):388–397. [PubMed: 17255259]
40. Duan H, Xiang H, Ma L, Boxer LM. Functional long-range interactions of the IgH 3' enhancers with the bcl-2 promoter region in t(14;18) lymphoma cells. Oncogene. 2008 Dec 4; 27(53):6720–6728. [PubMed: 18695675]

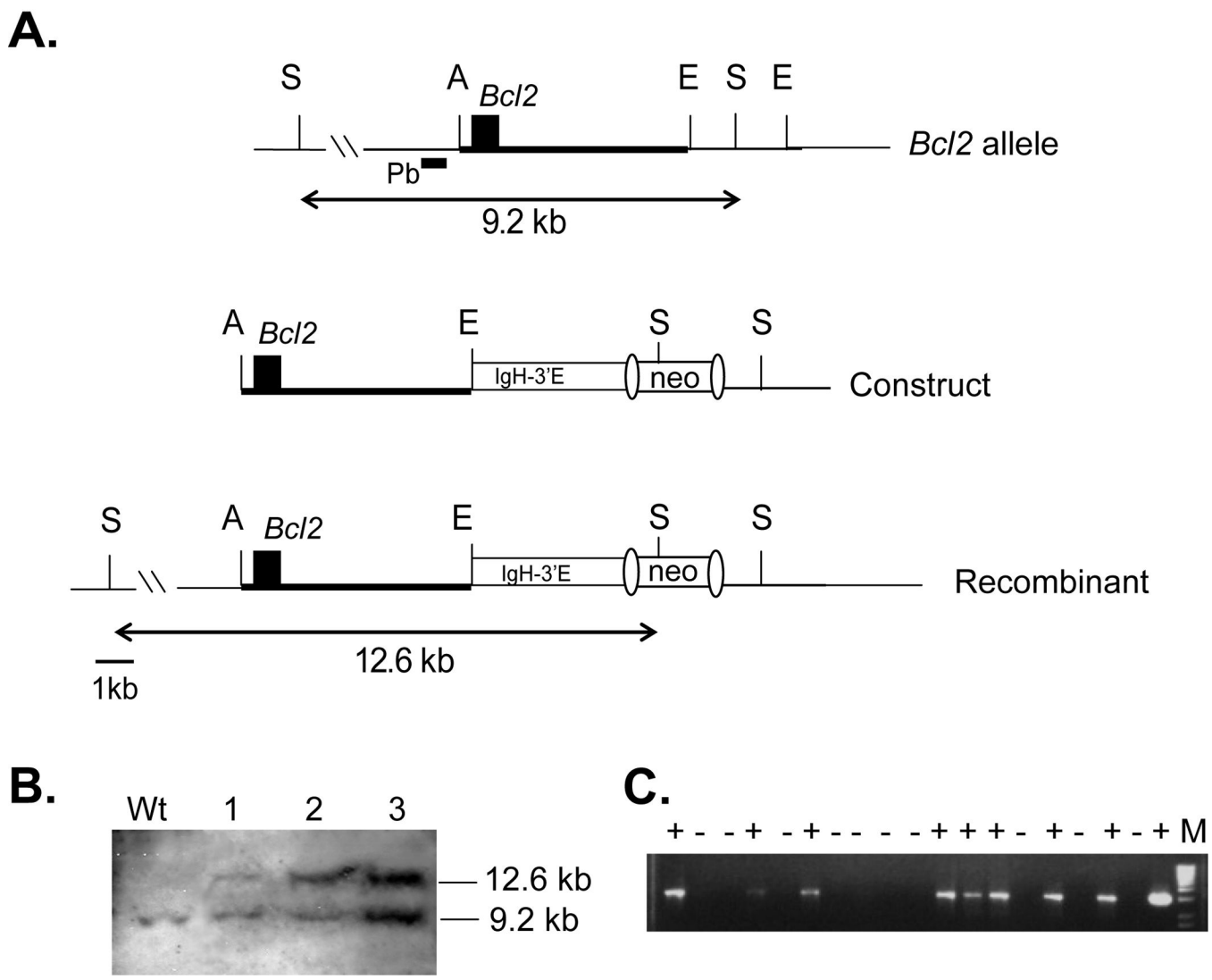

Figure 1. Targeting of the IgH 3'-enhancers (IgH-3'E) to the *bcl*-2 locus

A. Diagram of the murine *Bcl2* genomic locus (top), the targeting construct (middle), and the neomycin (neo)-IgH-3'E-bcl2 knock-in allele (bottom). The IgH 3'enhancers are located immediately 3' of the *Bcl2* 3' UTR. It is important to note that there is a large intron present in the mouse *Bcl2* gene, and the distance from the *Igh* enhancers is approximately 170 kb to the *Bcl2* promoter. The probe (Pb) used to identify recombination in Southern analysis is shown, and the loxP sites are indicated as ovals. A: AseI; E: EcoRI; S: SpeI. **B.** Southern blot analysis of SpeI-digested genomic DNA with the probe shown in A. The genomic DNA is from wild-type ES cells (Wt), and three heterozygous neomycin-IgH-3'E-bcl2 knock-in ES cell clones (1, 2 and 3). The wild-type allele is 9.2 kb, and the knock-in allele is 12.6 kb. **C.** Long distance PCR analysis of mouse tail DNA from neomycin-IgH-3'E-bcl2 mice. One primer is from the mouse *bcl*-2 region and the other primer is from the neomycin cassette. The amplified 3.0 kb PCR fragment on agarose gel indicates neomycin-IgH-3'E-bcl2 mice.

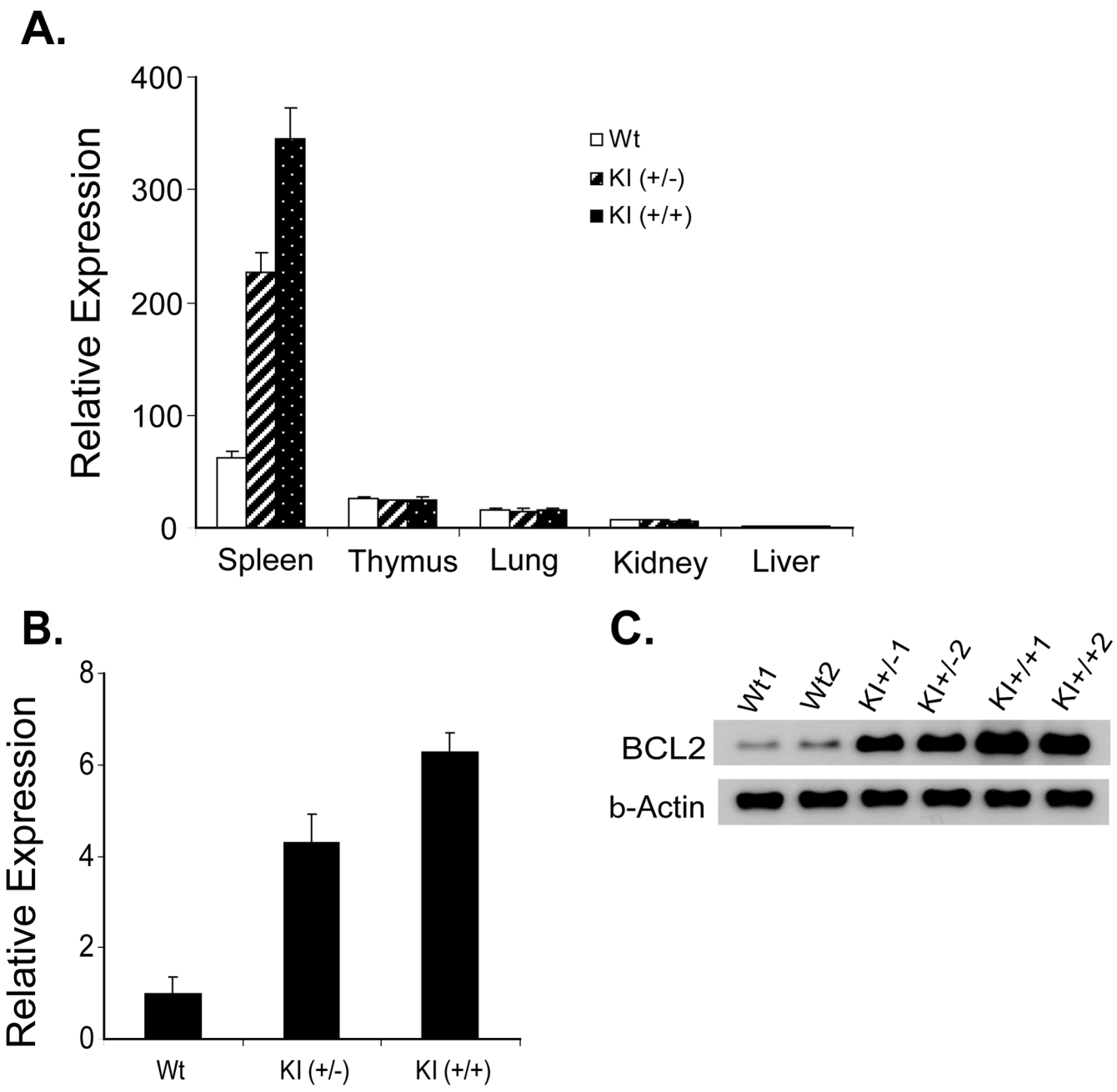

Figure 2. Increased *Bcl2* mRNA and protein in B cells from IgH-3'E-bcl2 mice

A. Tissue-specific expression of *Bcl2* driven by the *Igh* 3' enhancers in IgH-3'E-bcl2 mice. RNA was prepared from spleen, thymus, lung, kidney and liver of three IgH-3'E-bcl2 heterozygous (KI+/−), three IgH-3'E-bcl2 homozygous (KI+/+) and four wild-type (Wt) mice. **B.** *Bcl2* mRNA expression in splenic B cells from three wild-type (Wt) mice, three IgH-3'E-bcl2 heterozygous (KI+/−), and three homozygous (KI+/+) mice. Real-time RT-PCR was performed to analyze total *Bcl2* mRNA, and GAPDH was used as the control for normalization. **C.** Western blot analysis of BCL2 protein expression in splenic B cells from

wild-type (Wt), IgH-3'E-bcl2 heterozygous (KI+/−), and homozygous (KI+/+) mice. The loading control was β-Actin. All mice were 2 months of age.

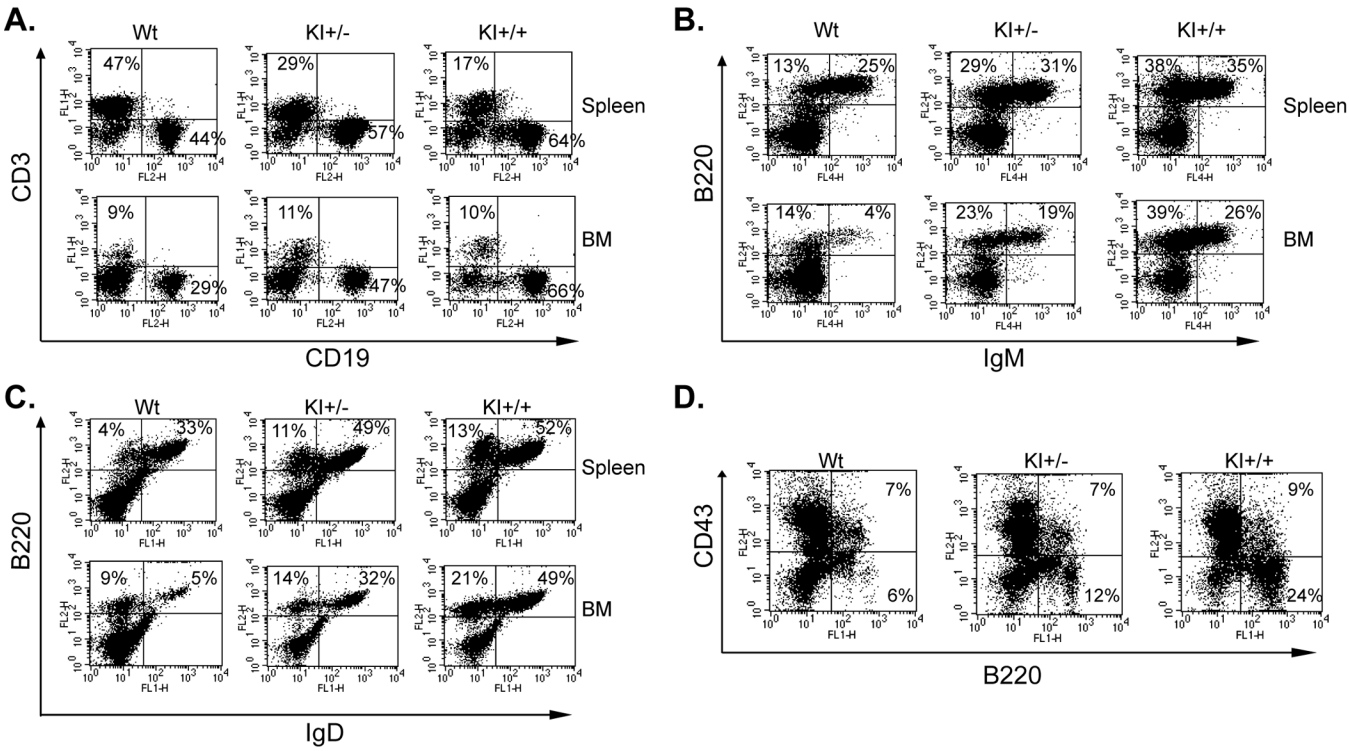

Figure 3. Accumulation of pre-B cells (B220^{+} CD43^{-} IgM^{-}) and mature B cells in young (2 mo) IgH-3'E-bcl2 mice

A. Single-cell suspensions were prepared from bone marrow (BM) and spleen of young heterozygous IgH-3'E-bcl2 mice (KI+/−), homozygous IgH-3'E-bcl2 mice (KI+/+), and age-matched wild-type (Wt) littermates. Cells were stained with antibodies to CD3 and CD19. The percentage of cells in each quadrant region is shown. **B.** Cells from BM and spleen were stained with antibodies to B220 and IgM and analyzed by flow cytometry. **C.** Cells from BM and spleen were stained with antibodies to B220 and IgD and analyzed by flow cytometry. **D.** Analysis of pro-B and pre-B cells in the bone marrow of IgH-3'E-bcl2 mice. Cells from bone marrow were stained with PE-, FITC- or APC-conjugated antibodies to B220, CD43, and IgM. The IgM positive cells were gated out.

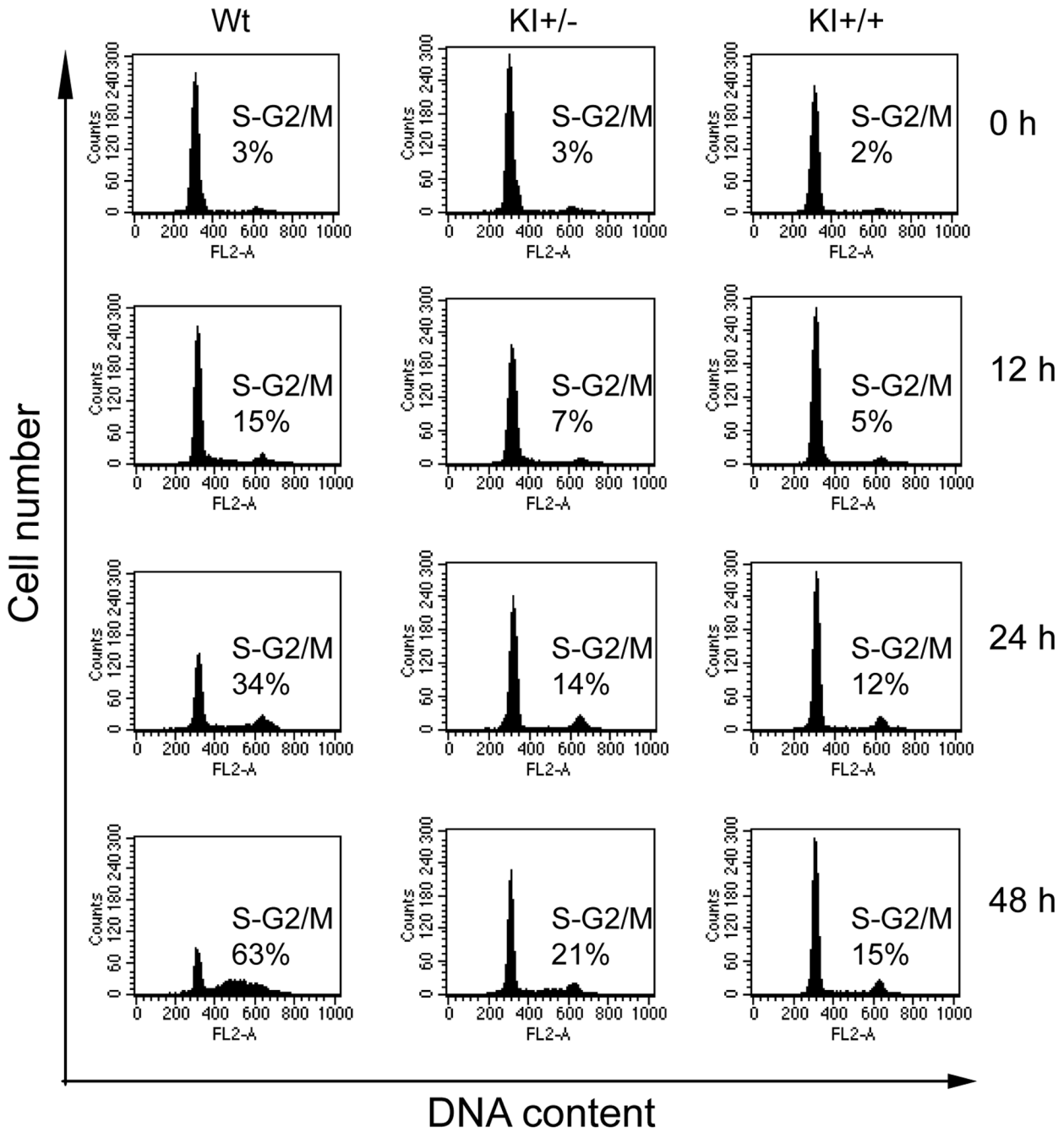

Figure 4. Over-expressed Bcl-2 in splenic B cells of IgH-3'E-bcl2 mice delays the transition from G0/G1 to S-G2/M phases of the cell cycle

Purified B cells from spleen were treated with anti-CD40 (5 μg/ml) for 0, 12, 24, and 48 h. The cells were collected at the indicated times stained with propidium iodide and analyzed by flow cytometry. The data shown are representative of three independent experiments comparing B cells from wild-type (Wt) littermate controls, heterozygous IgH-3'E-bcl2 mice (KI+/−), and homozygous IgH-3'E-bcl2 mice (KI+/+). Mice were 2 months of age.

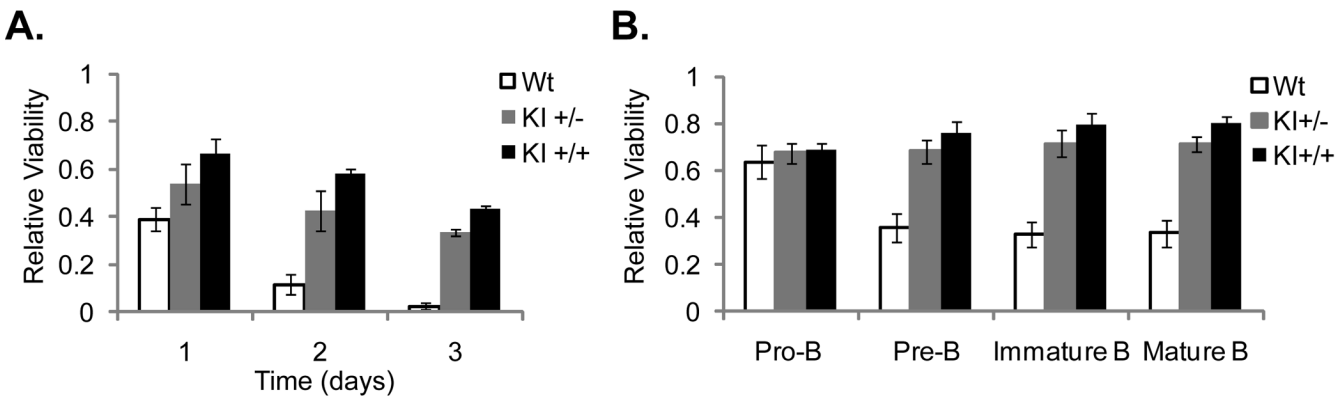

Figure 5. B cells from IgH-3'E-bcl2 mice show increased viability

A. B cells were isolated from the spleens of 6–8 month old wild-type (Wt), heterozygous IgH-3'E-bcl2 mice (KI+/−), and homozygous IgH-3'E-bcl2 mice (KI+/+) and cultured for the indicated times. Cell viability was determined using a colorimetric MTT assay. The data represent the mean ± SD of at least three determinations (*n = 3*, triplicate for each mouse) and viability relative to the time of isolation is shown. **B.** Single-cell suspensions were isolated from the bone marrow (BM, pro-B- and pre-B-cells) and spleen (immature and mature B cells) of young wild-type mice (Wt), heterozygous IgH-3'E-bcl2 mice (KI+/−), and homozygous IgH-3'E-bcl2 mice (KI+/+). Cell viability was determined using 7-ADD in the presence of antibodies to B220, CD43, IgM and IgD to identify specific B cell subsets by flow cytometry. Viability was normalized to the time of isolation (0 hours) and relative viability after 24 hours in culture is shown (*n=3*).

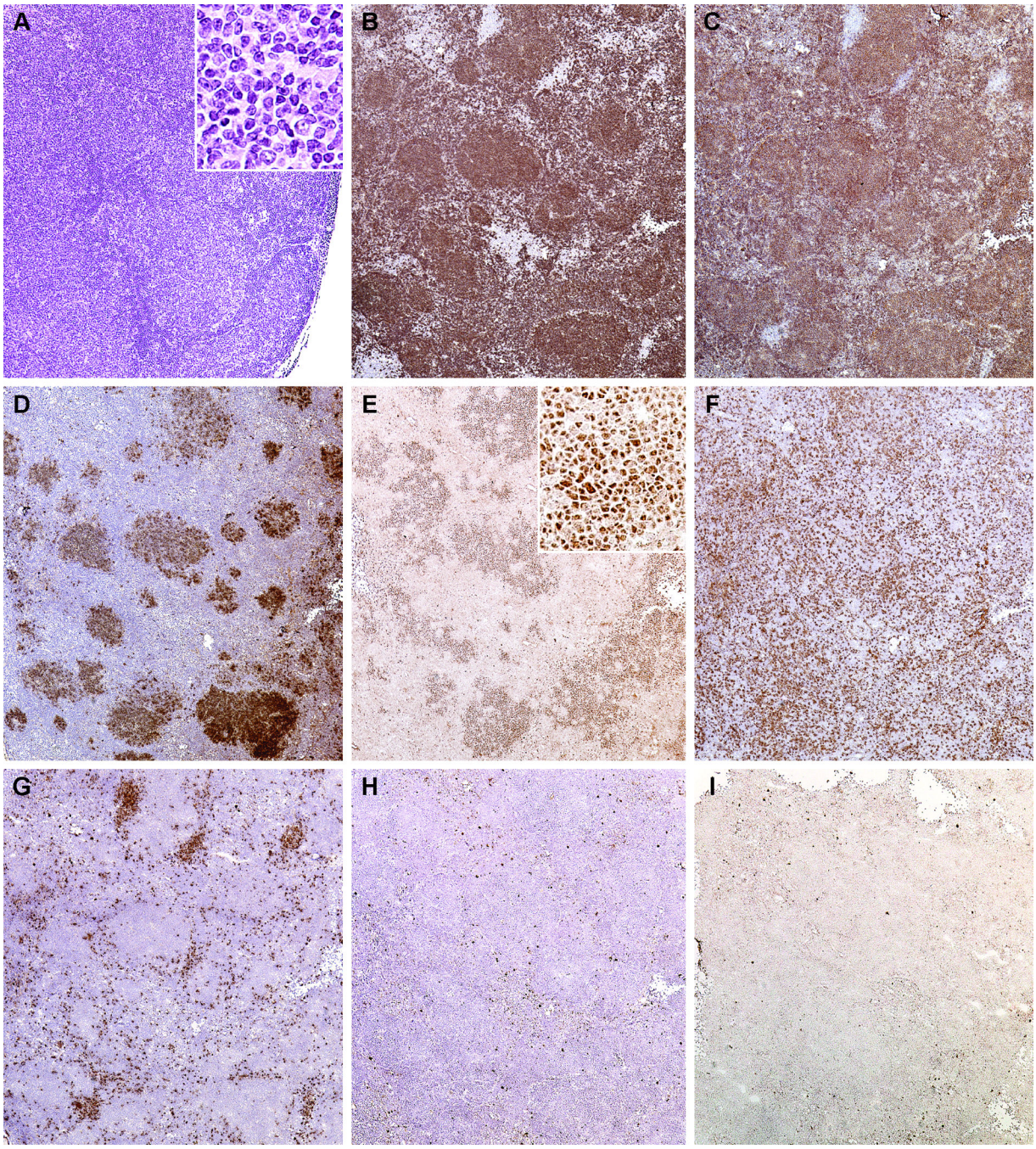

Figure 6. IgH-3'E-bcl2 mice develop follicular B cell lymphoma

A. H&E-stained section of a lymph node from a 7 month old IgH-3'E-bcl2 mouse shows complete effacement of the nodal architecture by a follicular lymphoma. The follicles contain many small-cleaved cells with irregular nuclear outlines, hyperchromatic chromatin and small nucleoli (inset). **B–I.** The lymphoma expresses B cell antigens (**B.** CD45R/B220 and **C.** CD19) and germinal center markers (**D.** PNA binding and **E.** BCL6 nuclear expression). There are scattered T cells (**F.** $CD4^+$ > **G.** $CD8^+$) in and around the follicles. Follicular dendritic cells were found in many of the follicles (not shown). **H,I.** There was no

specific staining with the negative control antibodies. (**A.** H&E-stained formalin-fixed paraffin-embedded section, original magnification 100×; inset original magnification 400×. Results are representative of 20 knock-in mice, from 7 to 14 months of age. **B–I**. Semi-serial frozen sections stained with rat mAb to **B.** CD45R/B220, **C.** CD19, **F.** CD4, **G.** CD8, or **H.** irrelevant negative control antigen, with rabbit polyclonal antibody to **E.** bcl6 or with **I**. normal rabbit serum, or with **D.** PNA. **B–I**. Immunoperoxidase/DAB stain (brown) with **B–D**, **F–H**. hematoxylin counterstain (purple) or **E, I.** no counterstain. Original magnification 100×; inset **E**, original magnification 300×. Results are representative of 6 knock-in mice, from 7 to 14 months of age. For comparison, please see Supplementary Figure 1 for immunoperoxidase/DAB stains of lymph node from an 11 month old Wt mouse).

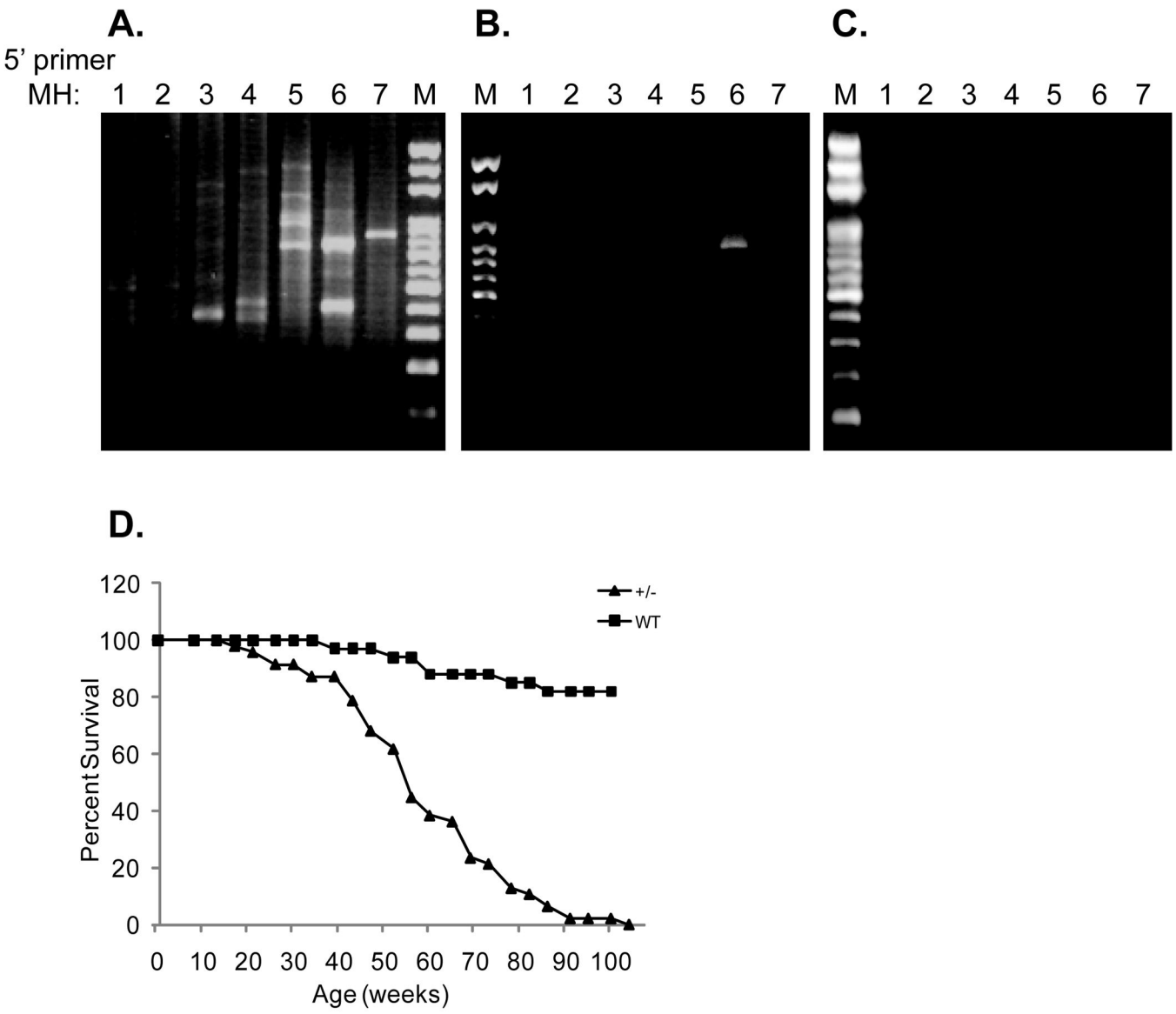

Figure 7. Clonality analysis of lymphomas in IgH-3'E-bcl2 mice

A–C. PCR analysis of clonality in IgH-3'E-bcl2 mice. Lanes MH1-MH7 represent second round PCR from amplification with individual degenerate primers MH1-7 and 3' primer JHR, run alongside a 100bp molecular weight marker (M). **A.** DNA from splenic B cells of wild-type mice was used as control. **B–C.** DNA from clonal B cells in lymphomas of heterozygous IgH-3'E-bcl2 mice. **D.** Survival plots of heterozygous IgH-3'E-bcl2 mice (+/−, *n*=47), and wild-type littermates (Wt, *n*=35).

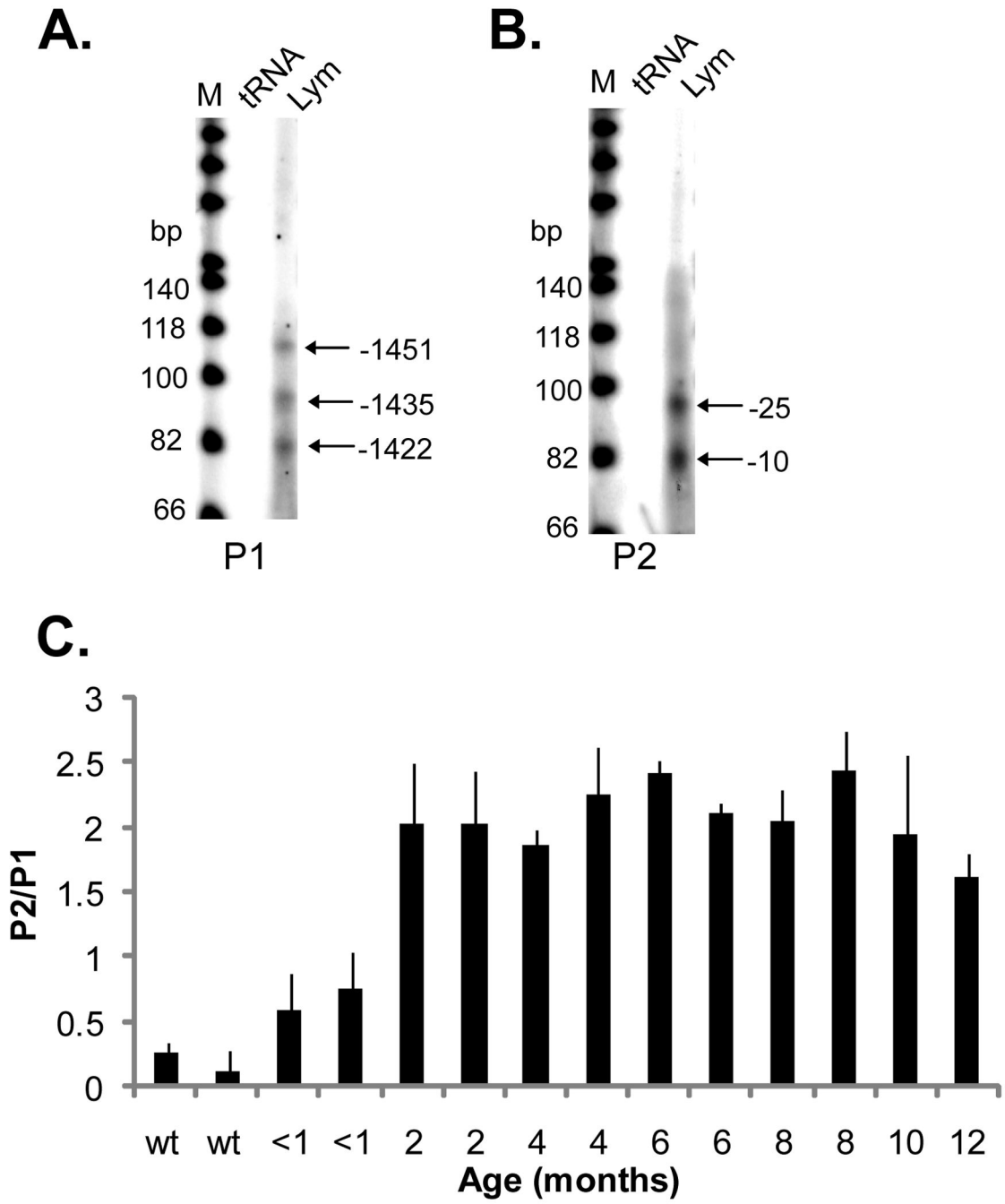

Figure 8. Analysis of the relative *Bcl2* promoter usage in lymphomas from homozygous IgH-3'E-bcl2 mice

A. Determination of the transcription start sites of the murine *Bcl2* P1 promoter by primer extension analysis. Arrowheads mark the transcripts, and their position relative to the ATG is shown. **B.** Determination of the transcription start sites of the murine *bcl*-2 P2 promoter as described for A. **C.** *Bcl2* promoter shift analysis in B cells from wild-type (Wt) and homozygous IgH-3'E-bcl2 mice at indicated ages in months. The *Bcl2* transcripts from the P1 promoter and the total (P1 + P2) transcripts were determined by real-time PCR and the

ratio of P2/P1 is represented on the y-axis. Quantification of transcripts initiating from the P2 promoter was determined by digital PCR.

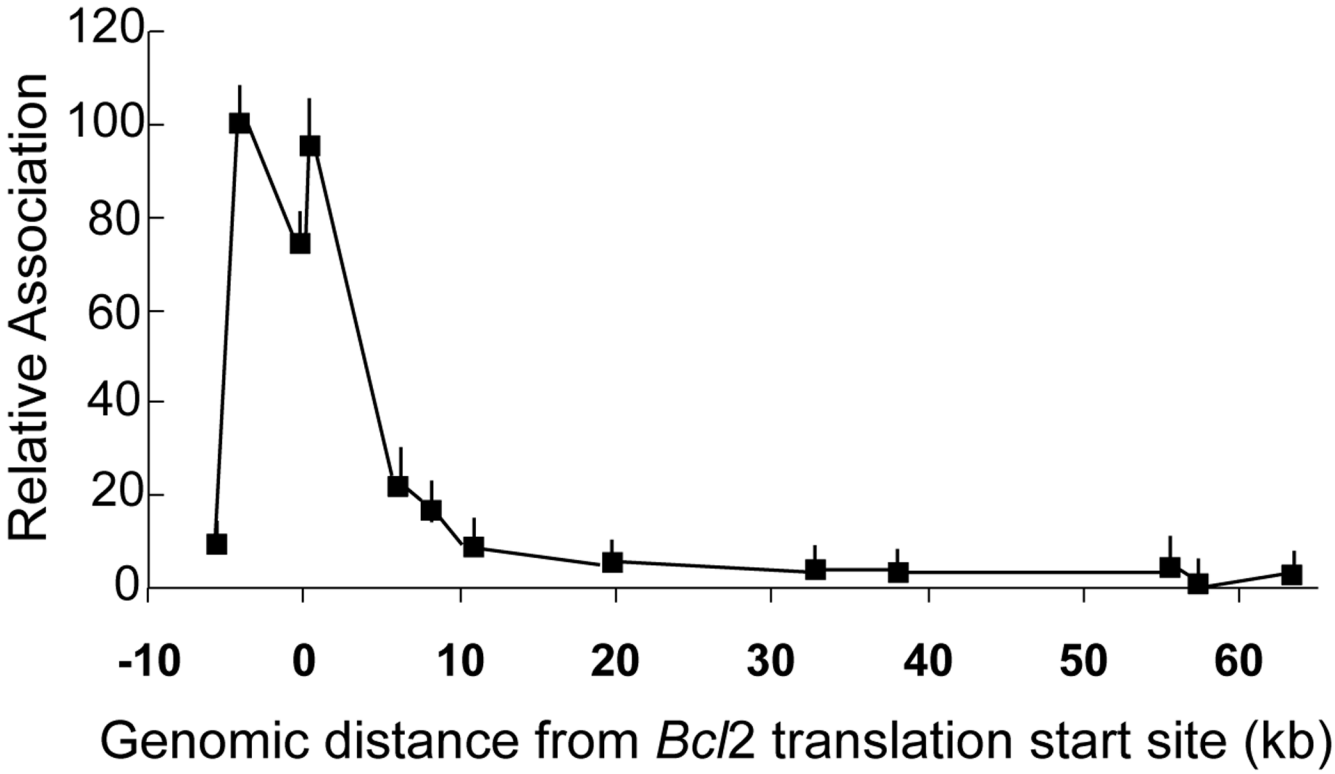

Figure 9. Spatial associations of the IgH 3' enhancers with the *Bcl2* promoter region in lymphoma cells from IgH-3'E-bcl2 mice determined by chromosome conformation capture

Lymphoma cells from heterozygous IgH-3'E-bcl2 mice were purified and used in 3C analysis. BamHI was used to digest the formaldehyde fixed chromatin. The anchor primer and probe were located in the *Igh* locus and the other set of primers were located in the *Bcl2* locus, 5' and 3' of the translation start site (defined as 0). Hybrid 3C fragments were quantified by real-time PCR and normalized for primer/probe efficiency using a control 3C template generated from equal molar PCR fragments using homologous PCR primers and to the association of BamHI sites in the Errc3 locus. The relative association shown is the average and standard deviation from three independent 3C analyses. The x-axis represents the genomic distance from the *Bcl2* translation start site, which was set to 0.

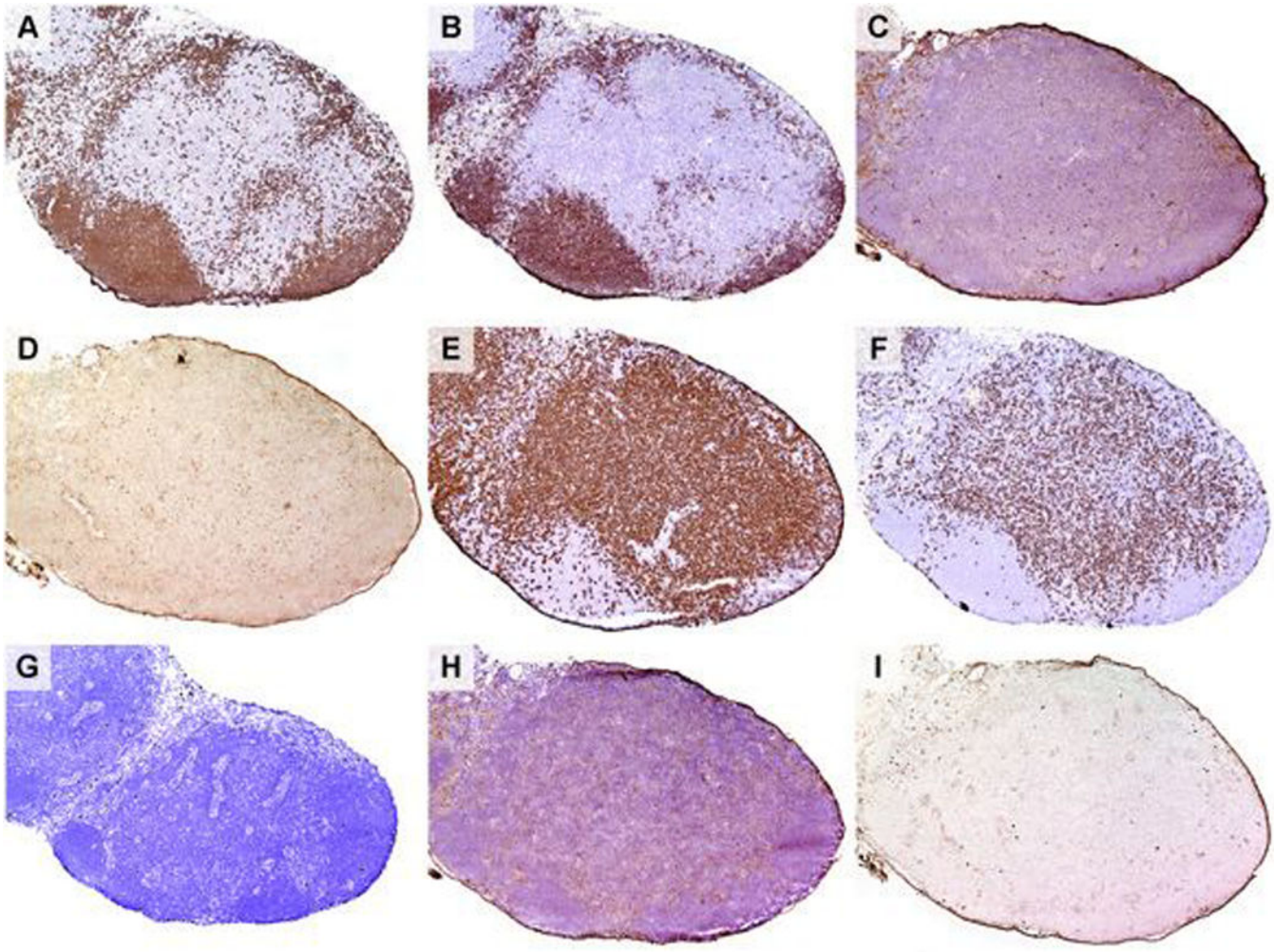

Figure 10.